COMPARISON OF THE SOLUTE (NITRATES) TRANSPORT THROUGH TWO TYPES OF SOIL PROFILES USING 1-D HYDRUS SOFTWARE

Lucia Balejčíková*

Nitrates, used especially in agricultural activities, are still a widespread risk for human health when exceeding recommended limits in various water drinking sources. Leaching of nitrates from soil to groundwater depends on various factors (as soil properties, the size of soil particles, the ability of specific soil components and plant to absorb water and nitrates, meteorological conditions). The main goal of the presented work was to show nitrates leaching through different soil types. Different solute transport processes and solute distribution in the soil profile were demonstrated using HYDRUS-1D model simulation. This mathematical computation research could contribute to the set-up of suitable fertilizers concentration applied in agriculture on the soil surface with defined hydraulic properties. This method represents the economically advantageous and simple first step before fertilizers application. Particularly, the main idea of such theoretical simulations is a timely environmental measures implementation against groundwater contamination.

KEY WORDS: soil profile, hydraulic properties, solute transport, mathematical simulation

Introduction

Nitrates are naturally occurring ions featured in the natural nitrogen cycle. Within fertilizers, composition creates support for crop growth in agriculture, which produce the main sources for human nutrition. Together with human consumption rate and growth, increased fertilization irrigation with domestic wastewater and changes in land-use patterns caused widespread pollution of drinking water sources by nitrates. Mobile ions easily pass through the soils and reach the aquifer (Balejčíková et al., 2020). This serious environmental problem still exists in many parts of the world. The main risk areas include South America, most European countries, the Eastern part of Africa, India and Australia (Zhou, 2015). In Slovakia, the situation with nitrates level is stabilized thanks to applied legislation, although there increased concentrations were measured by monitoring (Balejčíková et al., 2020). Fig. 1 shows a map of Slovakia with risk regions from 2019.

The main problem is associated with nitrates limits in relationship with organism and water sources used for drinking purposes. Higher-level over 50 mg l^{-1} and over 10 mg l^{-1} for infants (recommended by WHO and included in EU countries legislative) are linked with methaemoglobinaemia, the blue-baby syndrome development leading often to death (Greer and Shannon, 2005), and with the possible formation of n-nitroso compounds, potential carcinogens in the digestive tract.

The precise mechanism is unknown, probably the most important role plays the interaction between haemoglobin and various enzymes and nitrosamines (Gushgari and Halden, 2018). Also, the recent study aimed at the finding of the reason for patients mortality infected by the SARS-CoV-2 virus observed higher concentrations of nitrates post-mortal occurring (Lorentea et al., *in press*). This finding even more emphasizes the reasons for dealing with nitrates hydrological research. For nitrates to remove or concentration decreasing to acceptable health levels it is necessary to develop a suitable method for drinking water treatment (e.g. chemical reduction, reverse osmosis, electrodialysis, ion exchange, biological reduction, nanomagnetic separation or nanofiltration) (Kapoor and Viraraghavan, 1997; Soares, 2000; Shrimali and Singh, 2001; Bhatnagar and Sillanpää, 2011; Archna et al., 2012; Anand et al., 2018; Madhura et al., 2019;). When we take into account costs used for any separation technique applying, still it is advantageous to eliminate and economically manipulate with fertilization. Set-up of the initial concentration of nitrates in fertilizers applied on some soil surface is related to pre-determination of hydro-pedological and physico-chemical characteristics of the specific soil type, presence of cracks, denitrification bacteria, plant cover type, phenology and meteorological conditions. Fertilizer manufacturer takes into account surface and does not list all factors affecting transport processes of nitrates in the soil. Climate change
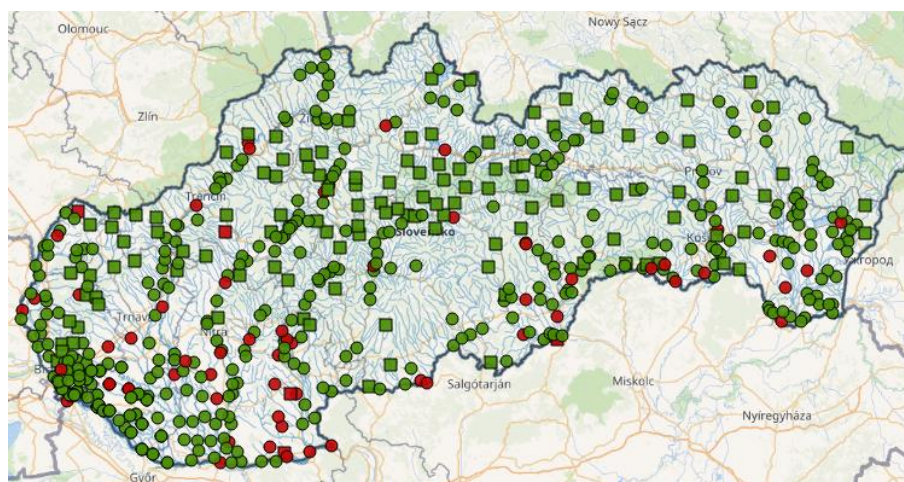
Fig. 1.   *The map of Slovakia with red marked points represented nitrates concentration over 50 mg l^-1 from monitoring data of 2019 (the figure taken from a public source of www.shmu.sk).*

affects the hydrological cycle, groundwater levels, resources and transport processes of various substances. Precise consequences of climate variations on the nitrate leaching to groundwater are not yet well enough understood (Stuart et al., 2011). The impacts of these changes are still difficult to predict, so it is necessary to deal with monitoring studies and the development of model scenarios to understand the impact of all factors on nitrate transport and leaching. The main goal of the study is the application of HYDRUS-1D software on 2 types of soil profile, occurring in the East Slovak Lowland. Numerical simulation using HYDRUS software allows to model the transport, distribution and leaching of water and dissolved nitrates. Theoretical calculation could be eventually compared with field data from the experiment and help to find all factors contributing to transport processes.

Methods

HYDRUS-1D computation

The HYDRUS-1D program was based on the one-dimensional Richards equation to simulate water and solute movement in variably saturated media, and the equation was solved by numerical method (Šimůnek et al., 2005). Richards equation (1) describes the basic water movement:

$$\frac{\partial \theta(h,t)}{\partial t} = \frac{\partial}{\partial z}\left[K(h)\left(\frac{\partial h}{\partial z} + 1\right)\right] \tag{1}$$

where
h – soil water pressure head [l],
θ – volumetric water content [cm^3 cm^{-3}],
t – time [days, d],
z – vertical coordinate [cm] with the origin at the soil surface (positive upward),
$K(h)$ – unsaturated hydraulic conductivity [cm d^{-1}].

The one-dimensional Hydrus-1D computer program (Šimůnek et al., 2008) was selected to simulate nitrates movement through the soil profile in the vertical direction. The Hydrus-1D program numerically solves the Richards equation for saturated and unsaturated water flow and the convection-dispersion equations for heat and solute transport. The governing one-dimensional solute flow equation for a partially saturated porous medium is described using the modified form (2) of the Richards equation:

$$\frac{\partial(\theta.C)}{\partial t} = \frac{\partial}{\partial z}\left[\theta.D\left(\frac{\partial C}{\partial z}\right)\right] - \frac{\partial(q.C)}{\partial z} + S_C \tag{2}$$

Initial and boundary condition are:

$C = C_0(z)$ at $-100 \le z \le 0$, $t=0$,
$\frac{\partial C}{\partial z} = 0, at\ z = -100, t>0,$

where
C – NO$_3$-N concentration in the soil solution [mg l^{-1}],
D – effective dispersion coefficient of the soil matrix [cm^2 d^{-1}],
S_c – sink term that includes mineralization, microbial immobilization and denitrification:
$S_c = S \times C_r + k_{min} - k_{im} \times C - k_{den} \times C,$

where
S – plant water uptake [cm d^{-1}],
C_r – outflow nitrogen concentration that is a function of soil nitrogen concentration (C) and maximum root nitrogen uptake coefficient (C_{RM}),
k_{min} – mineralization rate constant [μg cm^{-3} d^{-1}],
k_{im} – microbial immobilization rate constant [d^{-1}],
k_{den} – denitrification rate constant [d^{-1}].

The boundary conditions (3) in the case of nitrogen application treatments are:

$$-\theta . D\left(\frac{\partial C}{\partial z}\right) + q . C = q_0 . C_0(t), at\, z = 0, t > 0 \qquad (3)$$

where

$C_0(t)$ – nitrogen application rate at different times.

The equation for advection-dispersion (4), which describes the solute transport in a variably saturated soil is:

$$\frac{\partial \rho S}{\partial t} + \frac{\partial \theta C}{\partial t} = \frac{\partial}{\partial z}\left\{\theta . D \frac{\partial C}{\partial z}\right\} - q \frac{\partial C}{\partial z} \qquad (4)$$

where

ρ – bulk soil density [g cm^{-3}],
C and S – solute concentrations in the liquid [g cm^{-3}] and solis [g g^{-1}] phases
$S = K_d C$ with K_d [cm^3 g^{-1}] is the partition coefficient,
z – spatial coordinate,
D – dispersion coefficient [cm^2 d^{-1}],
q – volumetric flux density [cm d^{-1}] (Kanzari et al., 2018).

Results and discussion

This study was aimed at numerical simulation of NO_3^- application in the situation of the early stage of the vegetation period when water and solute root uptake are minimized and thus neglected. The main goal of this computation was to highlight the difference in the vertical transport of NO_3^- through two various soil profiles. The representative comparative texture consisting of silty-loam and sandy soil was selected due to their occurrence in the East Slovak Lowland. The vertical depth of soil was chosen according to the height of monoliths in the lysimetric station in Petrovce nad Laborcom, Slovakia (Matusek et al., 2017). Precise soil texture was not obtained from field measurements, therefore this numerical computation was based on the theoretical general data. The selected difference in soil types allows using HYDRUS-1D to show significant changes in aqueous solute transport when we neglect other factors as nitrogen mineralization, (de)nitrification, salts and water uptake by root and meteorological conditions in the early stages of the vegetation period. Firstly, the main input used parameters of the HYDRUS-1D model were collected in Table 1.

In the Table 1, θ_r [cm^3 cm^{-3}] is saturated water content, θ_s [cm^3 cm^{-3}] is residual water content, α [cm^{-1}] and n are empirical parameters, K_s [cm d^{-1}] is saturated hydraulic conductivity, L is tortuosity parameter in the conductivity function, D [cm^2 d^{-1}] is dispersion coefficient, K_d [cm^3 g^{-1}] is distribution coefficient and ρ is bulk density of specific soil type [g cm^{-3}]. The main difference

Table 1.   **Parameter used at HYDRUS-1D numerical simulation**

Soil texture		Silty-loam soil	Sandy soil
Parameter	**Units**	**Values**	
Depth	[cm]	250	250
Number of layers	[-]	1	1
Simulation time	[days (d)]	30	30
Time steps	[-]	daily	daily
Hydraulic properties			
θ_r	[cm^3 cm^{-3}]	0.067	0.045
θ_s	[cm^3 cm^{-3}]	0.45	0.43
α	[cm^{-1}]	0.02	0.145
n	[-]	1.41	2.68
K_s	[cm d^{-1}]	10.8	712.8
L	[-]	0.5	0.5
Boundary conditions			
Water flow			
Upper boundary condition		Constant pressure head	
Lower boundary condition		Free drainage	
Solute transport			
Upper boundary condition		Concentration flux BC	
Lower boundary condition		Zero concentration gradient	
Solute transfer properties			
Layer	[cm]	0–250	0–250
D	[cm^{2}d^{-1}]	55	55
K_d	[cm^3 g^{-1}]	0.7	0.7
ρ	[g cm^{-3}]	1.33	1.7

between silty-loam and sandy soil comes from their different hydraulic properties, related to the structure of the porous system with different geometry, size and connectivity. The relationship between pressure head, h, and water content, θ, for silty loam (Fig. 2a) and sandy soil (Fig. 2b) shows the main effect of soil texture described by parameters in Table 1. Saturation in Fig. 2b is achieved at air-entry pressure.

The ability of soil to pass water through pore space can be demonstrated as a dependence of hydraulic capacity versus pressure head (Fig. 3a, b). Maximum capacity for sandy soil indicates the maximum amount of infiltration moisture in the soil subsurface illustrated in Fig. 3b.

The most important hydrogeological parameter, hydraulic conductivity, is affected by both soil and fluid properties and characterizes the ability of water and solute transport through characteristic soil profile due to hydraulic gradient. It depends on the soil pore geometry as well as the fluid viscosity and density. The hydraulic

conductivity for a given soil for example becomes lower when the fluid is more viscous than water. Saturation in our case was achieved for sandy soil at air-entry (h) value (Fig. 4b) in contrast to silty-loam profile (Fig. 4a). The main affecting parameter, in this case, is soil density associated with the soil texture.

Fig. 5 shows soil moisture (theta) at 40, 100 and 160 cm depth of layers within horizons below the ground surface divided according to the layout of lysimeter monoliths located in the East Slovak Lowland. 1-D profile with the hydraulic properties of silty-loam (Fig. 5a) and sandy soil (Fig. 5b) as a function of time shows the soil moisture (theta) response in a shorter time for sandy soil (Fig. 5b). Fig. 6 represents wetting profiles soil moisture (theta) distributions in depth. Different wetting profiles are related to variations in soil textures and thus fitting parameters for simulation applied on both soil types. Wetting front is achieved easier in the sandy soil profile (Fig. 6b). It should be noticed, that the wetting front
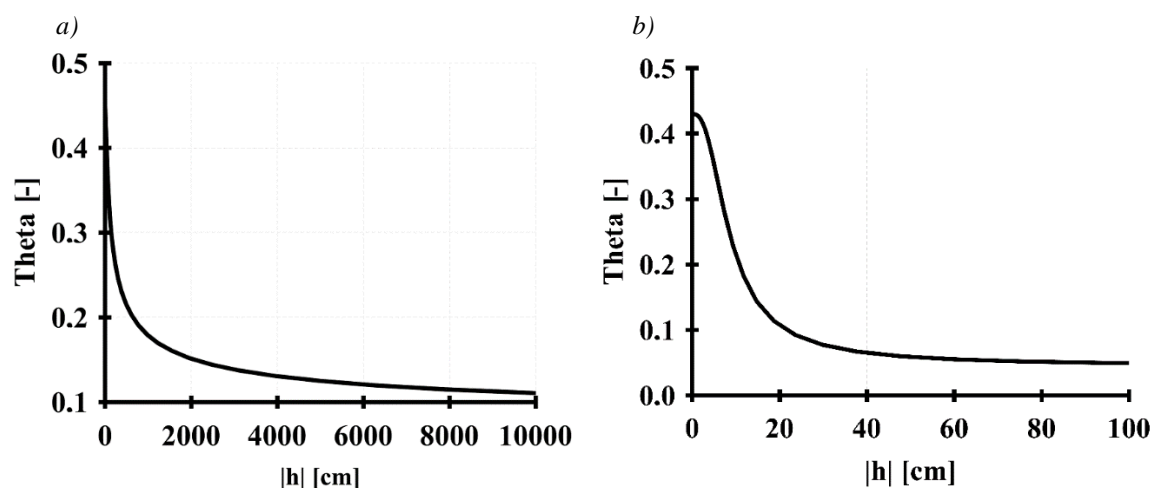

Fig. 2.   Simulated pressure head versus water content for a) silty-loam and b) sandy soil profile.
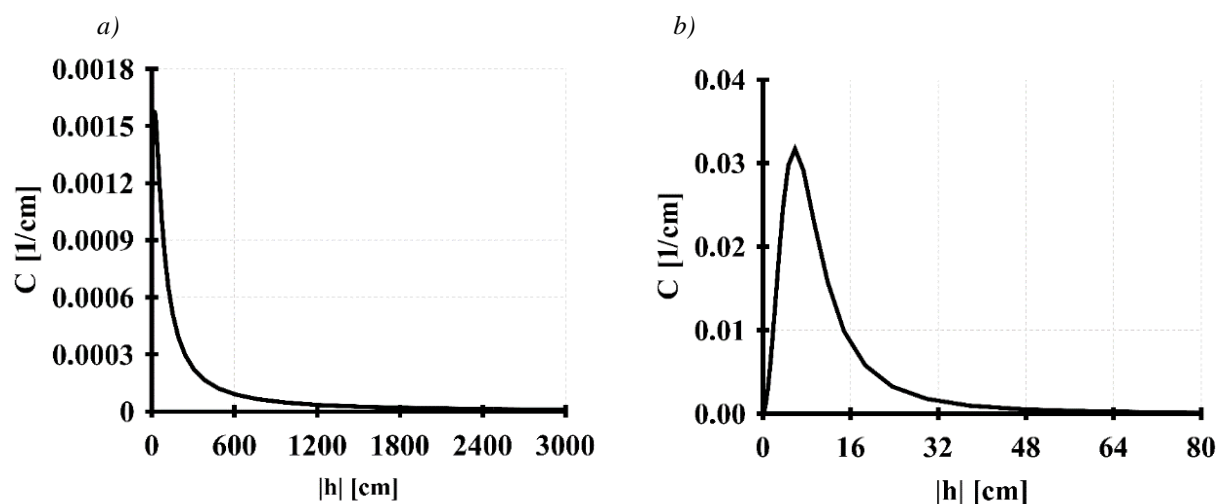

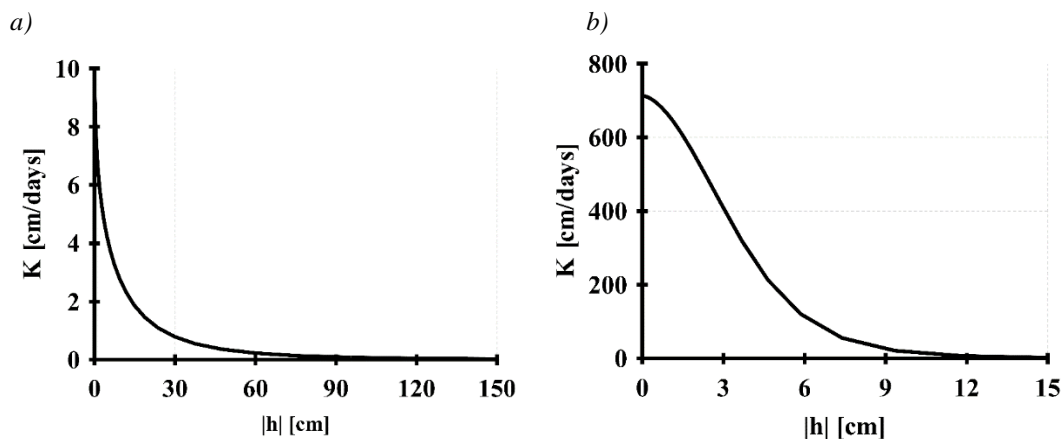*Fig. 3.   Simulated pressure head versus hydraulic capacity for a) silty-loam and b) sandy soil profile.*

Fig. 4.   *Simulated pressure head versus hydraulic conductivity for a) silty-loam and b) sandy soil profile.*
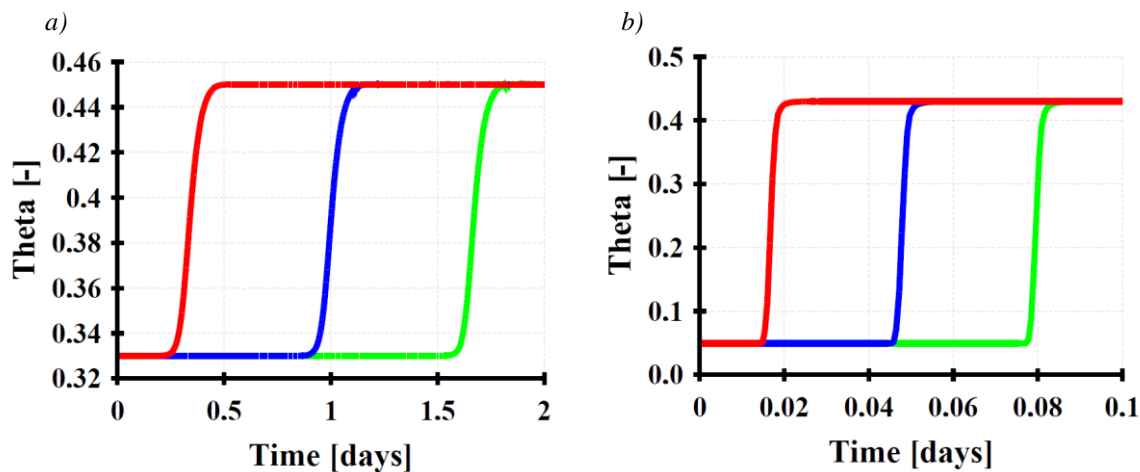

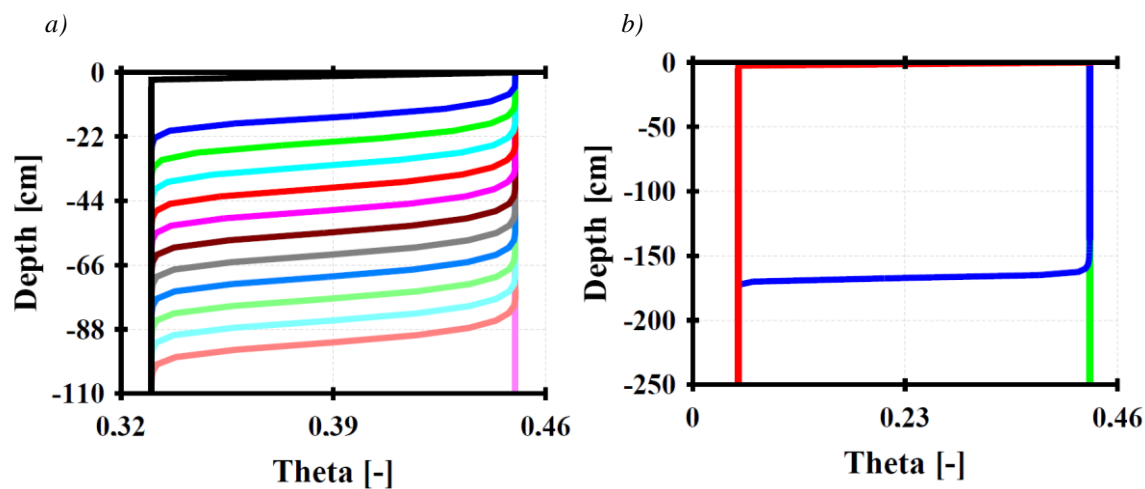Fig. 5.   *Soil moisture (theta) simulation in time for a) silty-loam and b) sandy soil profile.*

Fig. 6.   *Depths versus soil moisture (theta) simulation for a) silty-loam and b) sandy soil profile.*

for a sandy profile is very sharp (Fig. 6b) in comparison with the smoother wetting front for a silty-loam profile (Fig. 6a.) associated with finer-textured soil having relatively lower n and α values requiring coarser discretization. After water infiltration into the dry soil profile, water tends to approach the saturated water content. The wetting front changes from its initial low value to a value near saturation in a small distance (silty-loam soil – Fig. 6a) and high distance (sandy soil – Fig. 6b). The rate at which the wet front process with depth of wetting is about 8 times greater in the sandy soil profile.

Fig. 7 was constructed after concentrations set-up of applied solute (nitrates) according to the standard NO_3^- concentration (*i.e.* solute concentration = 0.003 mmol cm^{-3}) on the different soil profiles. This concen-

tration is recommended by the user manual of "Kristalon" grass fertilizer (producer AGRO CS a.s. the Czech Republic, originating in the Netherlands). The rate of solute transport throughout the sandy soil profile achieve a constant maximum concentration of 0.003 within ~ 1 day for all three observation points (40, 100 and 160 cm) in comparison with the silty-loam profile. The solute is transported about 50 times faster in the first layer (40 cm) for sandy soil than in the silty-loam soil profile. In the two next layers, the rate increased more than 100 times in the sandy soil against silty-loam soil.

Fig. 8 represents the similar 50 times increasing solute transport rate in the case of sandy soil in contrast to silty loam after 5 times higher solute initiation concen-tration (*i.e.* 0.016 mmol cm^{-3}) for the first layer (40 cm). Solute (nitrates) flow shows the symmetrical shape,
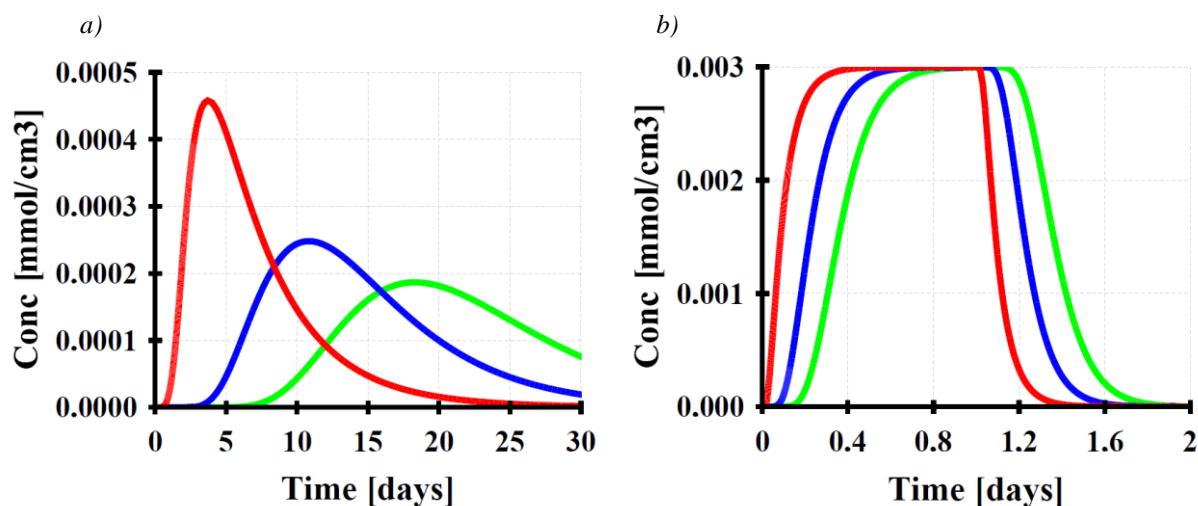

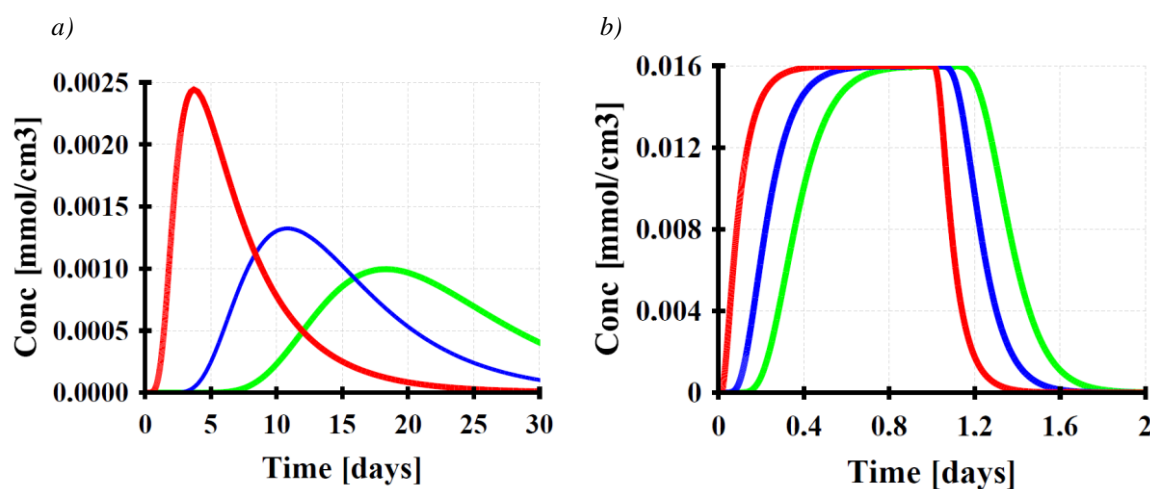Fig. 7.   *Solute concentration simulation in time for a) silty-loam and b) sandy soil profile.*

Fig. 8.   *Solute concentration simulation in time for a) silty-loam and b) sandy soil profile.*

demonstrating equilibrium behaviour in sandy loam soil column divided into 3 depth (observation points): 40, 100 and 160 cm (Fig. 8b).

Our numerical 1-D simulation demonstrates a significant difference in water and solute vertical flow through two different soil profiles. Silty-loam soil texture has better retention capacity in comparison with sandy soil.

Illustrations exported from 1-D HYDRUS numerical simulation could contribute to the economically and environmentally fertilizers application by the inclusion of soil type into the instructions for use of the fertilizer. Our results could be supported by the field experiments performed in a lysimetric station after summarization of all input specific parameters. Lysimeter monoliths could be the suitable experimental tool for the study of transport processes by applying fertilizers, nutrients, pesticides, colloids, pathogens or nanoparticles at the soil surface in real-time and real conditions and then by numerical computation predict especially the rate of contamination to the ensuring necessary measures for health and life protection. This simulation was aimed at soil fertilization in the early stage of the vegetation period when we neglect root water and nutrients up-take for plant growth. This article indirectly points to the fact, that during the vegetation period greater retention of water and solute in the case of fine soil texture (silty-loam) could lead to increasing of solute concentration, which plants are not able to take up together with water against the concentration gradient. The result is slower growth followed by wilting. Fertility will decrease. Faster leaching of nitrates through sandy soils creates another problem. Except for contamination of water sources provided for drinking, nitrates flow through drainage water to the rivers could cause algal overgrowth and eutrophication.

Conclusion

The present simulation study demonstrated the high impact of soil hydraulic properties on water and solute (nitrates) transport. We have shown about 50 times solute flow rate increasing for sandy soil compared to silty-loam in the first 40 cm layer of the soil profile. Nitrates move more than 100 times faster in the deeper layers 100 and 160 cm in sandy soil in contrast to silty-loam. This research aimed at numerical simulation of water and solute transport could be a suitable, quick and strong tool for the management of water and fertilization in agriculture to the protection of the health and life of the population. The study suggests reconsidering modification of the "instructions for use" of a given fertilizer distributed on the world market suitable for a given type of soil profile in a specific locality of the world. Reduction of economic and crop losses in advance could be high motivation. Another reason for using computation modelling is to estimate the rate of spread of a pollutant in the soil profile in the case of large-scale accident or industrial accident event and to take the necessary measures, warn people, stop the distribution of water resources for domestic use,

water purification, and animal protection). Preventive measures should be identified and these need to be derived through interdisciplinary including collaboration between regulators, the farming community, government departments and scientists.

Acknowledgement

References

Anand, A., Unnikrishnan, B., Mao, J.-Y., Lin, H.-J., Huang, C.-C. (2018): Graphene-based nanofiltration membranes for improving salt rejection, water flux and antifouling–A review. Desalination, vol. 429, 119–133.

Archna, Sharma, S. K., Sobti, R. C. (2012): Nitrate Removal from Ground Water: A Review. E-J Chem, vol. 9, no. 4, 1667–1675.

Balejčíková, L.; Tall, A.; Kandra, B.; Pavelková, D. (2020): Relationship of nitrates and nitrites in the water environment with humans and their activity. Acta Hydrologica Slovaca, 2020, vol. 21, 74–81.

Bhatnagar, A., Sillanpää, M. (2011): A review of emerging adsorbents for nitrate removal from water. Chemical Engineering Journal, vol. 168, 493–504.

Greer, F. R., Shannon, M. (2005): Infant methemoglobinemia: the role of dietary nitrate in food and water. Pediatrics, vol. 116, 784–786.

Gushgari, A. J, Halden, R. U. (2018): Critical review of major sources of human exposure to N-nitrosamines. Chemosphere, vol. 210, 1124–1136.

Kanzari, S., Nouna, B. B., Mariem, S. B., Rezig, M. (2018): Hydrus-1D model calibration and validation in various field conditions for simulating water flow and salts transport in a semi-arid region of Tunisia. Sustainable Environment Research vol. 28, 350–356.

Kapoor, A., Viraraghavan, T. (1997): Nitrate Removal From Drinking Water—Review. Journal of Environmental Engineering, vol. 123, 371–380.

Lorentea, L., Gómez-Bernal, F., Martín, M. M., Navarro-Gonzálvez, J. A., Argueso, M., Perez, A., Ramos-Gómez, L., Solé-Violán, J., Marcos y Ramos, J. A., Ojeda, N., Jiménez, A.: Working Group on COVID-19 Canary ICU. (2021): High serum nitrates levels in non-survivor COVID-19 patients. Medicina Intensiva, Available online 10 November 2020, In Press, Corrected Proof.

Madhura, L., Singh, S., Kanchi, S., Sabela, M., Bisetty, K., Inamuddin (2019): Nanotechnology-based water quality management for wastewater Treatment. Environmental Chemistry Letters, vol. 17, 65–121.

Matusek, I., Reth, S., Heerdt, C., Hrckova, K., Gubis, J., Tall, A. (2017): Review of lysimeter stations in Slovakia. 17. Gumpensteiner Lysimetertagung, 209–212, ISBN: 978-3-902849-45-8.

Shrimali, M., Singh, K. (2001): New methods of nitrate removal from water. Environmental Pollution, vol. 112, 351–359.

Soares, M. (2000): Biological Denitrification of Groundwater. Water, Air, & Soil Pollution, vol. 123, 183–193.

Stuart, M. E., Gooddy, D. C., Bloomfield, J. P., Williams, A. T. (2011): A review of the impact of climate change on future nitrate concentrations in groundwater of the UK. Science of the Total Environment, vol. 409, 2859–2873.

Šimůnek, J., van Genuchten, M. Th., Šejna, M. (2005): The HYDRUS-1D Software Package For Simulating The One-Dimensional Movement of Water, Heat and Multiple Solutes in Variably-saturated Media, Version 3.0. Department of Environmental Sciences, University of California Riverside, Riverside, California, USA.

Šimůnek, J., van Genuchten, M.T., Šejna, M. (2008): Development and applications of the Hydrus and STANMOD software packages, and related codes. Vadose Zone Journal, vol. 7, 587–600.

Zhou, Z. (2015): A Global Assessment of Nitrate Contamination in Groundwater. Internship report.

RNDr. Lucia Balejčíková, PhD. (*corresponding author, e-mail: balejcikova@uh.savba.sk)
Institute of Hydrology SAS
Dúbravská cesta 9
841 04 Bratislava
Slovak Republic